

Constructing FeTe₂ dot embed in N-doped carbon nanofibers composite as long-life and high-rate anode material for sodium-ion battery

Zihua Lin, Haiyan Zhang*, Changsheng Yang, Zhenjiang Liu, Daofeng Wen, Xiang Peng, Shengkai Li,

School of Materials and Energy, Guangdong University of Technology, Guangzhou, 510006, China.

Experimental

Materials synthesis

In short, this study began by dissolving 0.8 g of C₄H₇FeO₅·nH₂O and 1.5 g of polyacrylonitrile (PAN) in 10 mL of dimethylformamide (DMF), followed by 12 hours of stirring to create a homogeneous spinning solution. Various parameters were adjusted: the voltage, temperature, feeding rate, and the distance between the syringe needle and the collection device were set at 12 kV, 45°C, 0.045 mm/min, and 13 cm, respectively. Next, the precursor film obtained from this solution was subjected to a series of steps. It was initially dried overnight at 80°C and then stabilized in air for 90 minutes at 200°C, with a heating rate of 5°C minute⁻¹. Following this, the stabilized film was blended with tellurium powders in a 1:1 mass ratio and further annealed at 600°C for 5 hours, again with a heating rate of 5°C minute⁻¹. This annealing process was conducted within a tube furnace under a N₂ atmosphere. The end result was the creation of N-doped carbon fibers containing embedded FeTe₂ nanoparticles. For comparison, we also prepared Pure FeTe₂ through direct annealing and tellurization of iron acetate under

identical conditions but without the use of electrospinning. Additionally, bare carbon nanofibers (CNF) were produced through electrospinning PAN and subsequent annealing under the same conditions.

Materials characterization

The physical phases of the prepared samples were investigated by X-ray diffraction (XRD, Bruker D8 Advance, Germany). The morphology and internal structure of the samples were examined by field emission scanning electron microscopy (SEM, SU8010, Hitachi, Japan) and transmission electron microscopy (TEM, Talos F200S, FEI, Czech Republic). The elemental content of FeTe₂/CNFs was analyzed by x-ray energy spectrometry (EDS). The carbon content in FeTe₂/CNFs was analyzed by thermogravimetric analysis (TGA, DSC3+, Mettler Toledo, Switzerland) at a heating rate of 10 °C min⁻¹ from room temperature to 900 °C in air. X-ray photoelectron spectroscopy (XPS) testing was performed using a multifunctional photoelectron spectrometer (ESCALAB 250Xi, Thermo Fisher, USA). Raman spectra were collected using a miniature Raman spectrometer (Renishaw RM2000, UK) with a laser excitation wavelength of 532 nm.

Electrochemical Measurements

Firstly, a black electrode paste was created by mixing the active material (FeTe₂/CNFs), conductive material (acetylene black), and binder (polyvinylidene fluoride) with N-methyl-2-pyrrolidone solvent in an 8:1:1 mass ratio. This paste was uniformly applied onto copper foil and then vacuum-dried at 80 °C for 12 hours. Subsequently, the dried electrode material was cut into electrode disks with a 10 mm

diameter. Each electrode had an active material mass loading of 0.7-0.9 mg. The coin-type half-cells (CR2032) were assembled in an argon-filled glove box at room temperature, with a sodium metal sheet serving as the reference electrode. A glass fiber separator (Whatman, GF/D) was used, and the electrolyte employed was 1.0 M NaPF₆ in diglyme (100%). This study conducted constant current charge/discharge cycling and rate distribution tests over a voltage range of 0.01-3V using the LAND CT2001A Battery Test System. Additionally, cyclic voltammetry (CV) measurements were carried out on an electrochemical workstation with a scan rate ranging from 0.2 to 1.2 mV s⁻¹, while electrochemical impedance spectroscopy (EIS) measurements covered a frequency range from 0.01 Hz to 10 kHz.

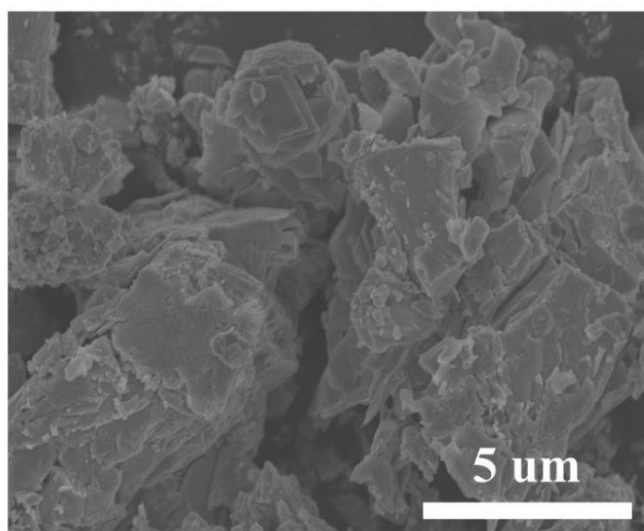


Fig. S1. SEM image of FeTe₂

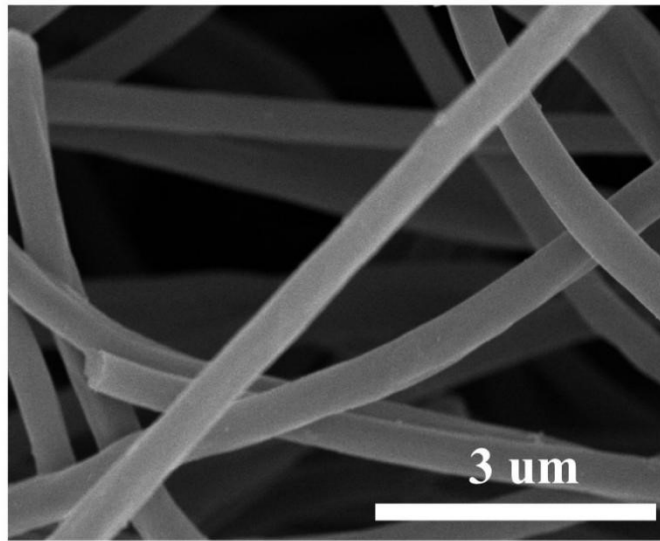


Fig. S2. SEM image of CNFs

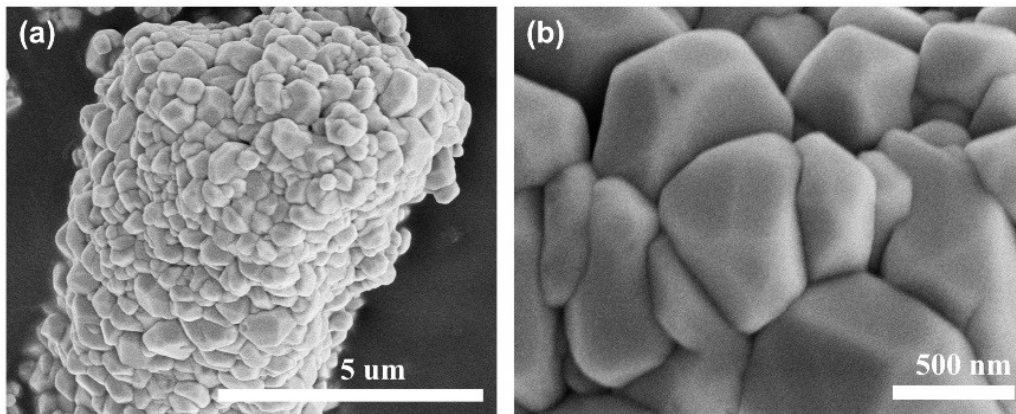


Fig. S3. (a-b) SEM image of tellurium powders

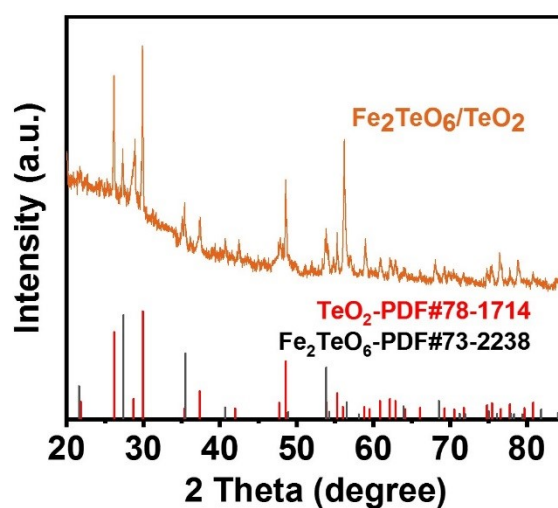


Fig. S4. XRD pattern of the product after heating $\text{FeTe}_2/\text{CNFs}$ in air to $650\text{ }^\circ\text{C}$

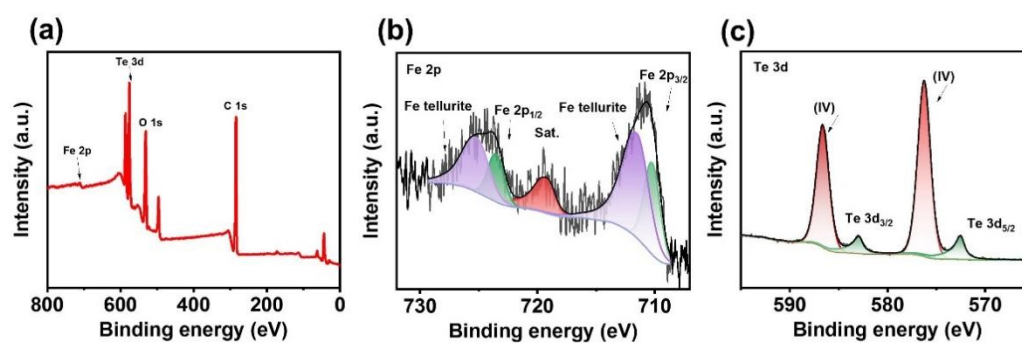


Fig. S5. (a) XPS total spectra of FeTe_2 . High-resolution XPS spectroscopy of (b) Fe 2p, (c) Te 3d.

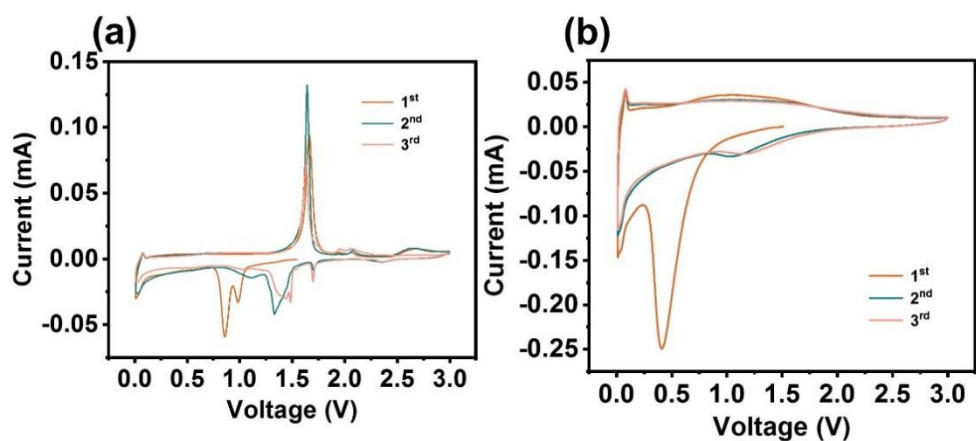


Fig. S6. (a) CV curves of FeTe₂ at 0.2 mV s⁻¹ in a voltage range of 0.01–3.0 V. (b) CV curves of CNFs at 0.2 mV s⁻¹ in a voltage range of 0.01–3.0 V.

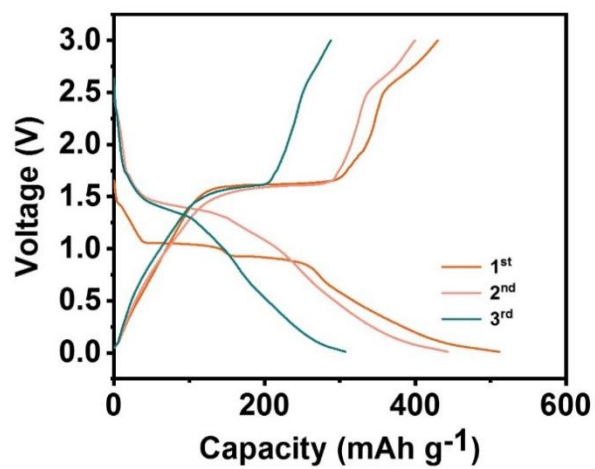


Fig. S7. Discharge/charge curves of FeTe₂ at 0.2 A g⁻¹.

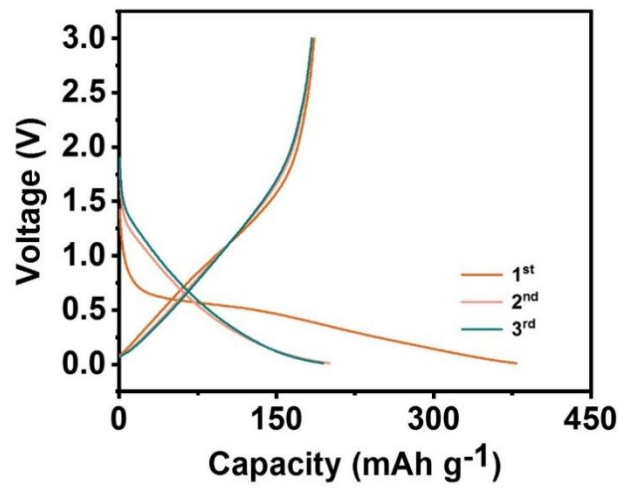


Fig. S8. Discharge/charge curves of CNFs at 0.2 A g⁻¹.

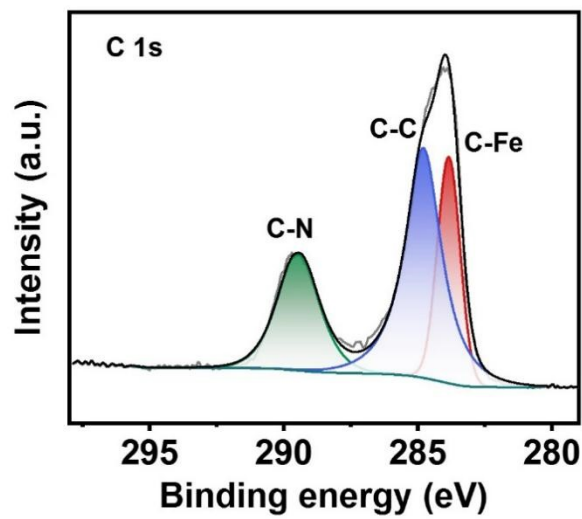


Fig. S9. the high-resolution C1s spectrum during the electrochemical process.

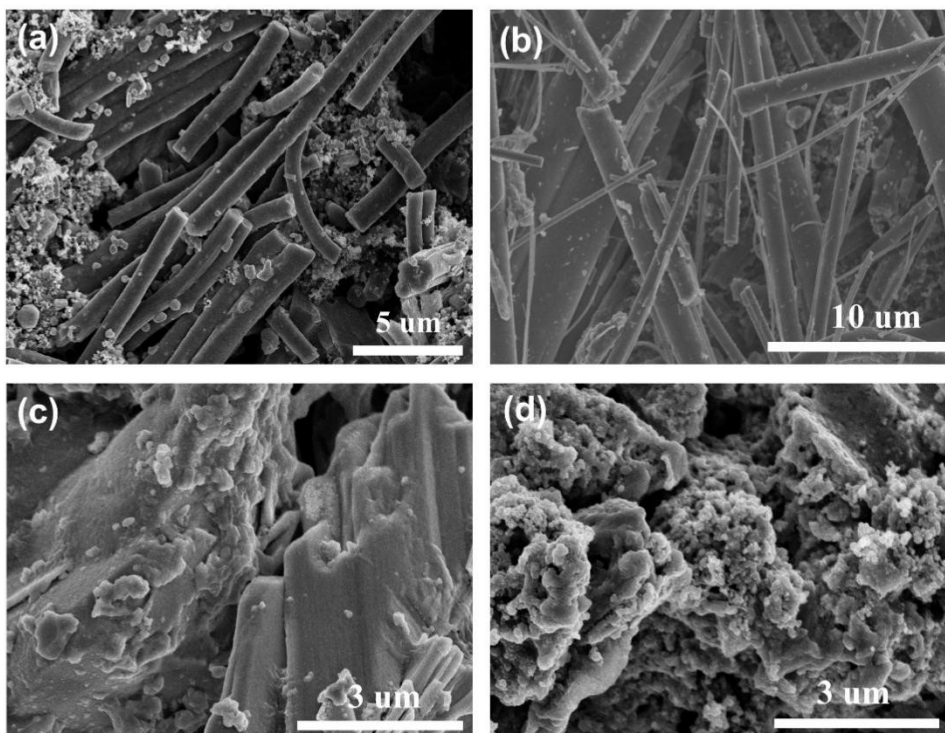


Fig. S10. (a) and (b) show the electron micrographs of the $\text{FeTe}_2/\text{CNFs}$ electrode before and after one hundred cycles. (c) and (d) show the electron micrographs of the FeTe_2 electrode before and after one hundred cycles.

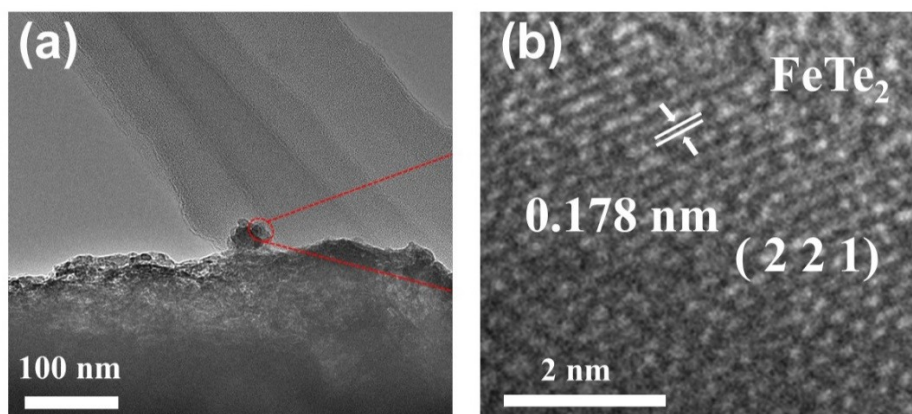


Fig. S11. (a) TEM images of $\text{FeTe}_2/\text{CNFs}$ electrode cycling for 50 cycles. (b) HRTEM images of $\text{FeTe}_2/\text{CNFs}$ electrode cycling for 50 cycles.

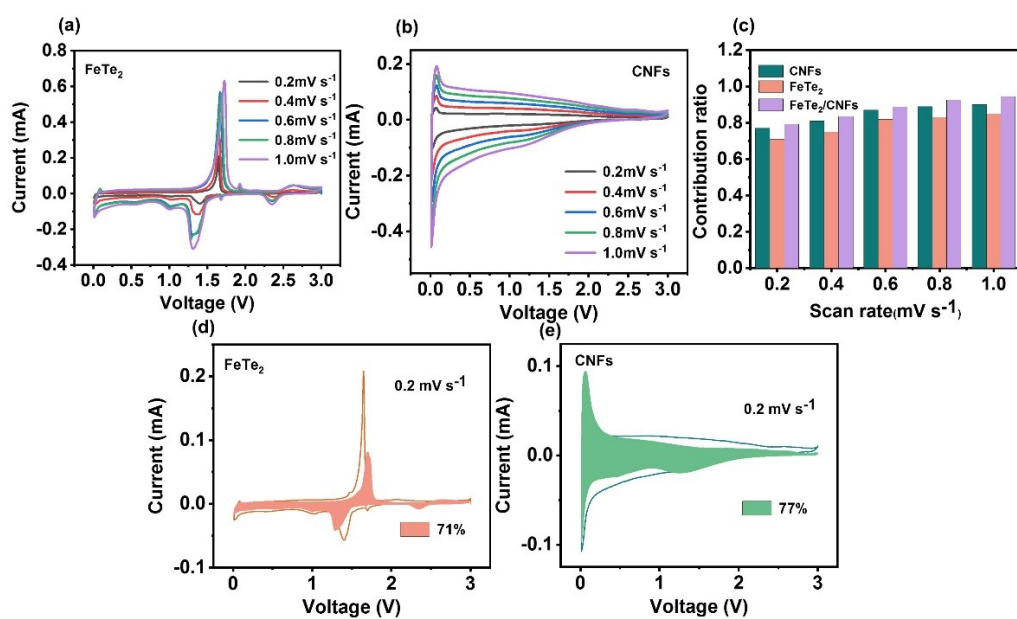


Fig. S12. (a-b) CV curves of FeTe₂ and CNFs at various scanning rates. (c) The ratio of capacitance contribution at various scan rates. (d-e) Pseudocapacitance contribution of FeTe₂ and CNFs at a scan rate of 0.2 mV s⁻¹.

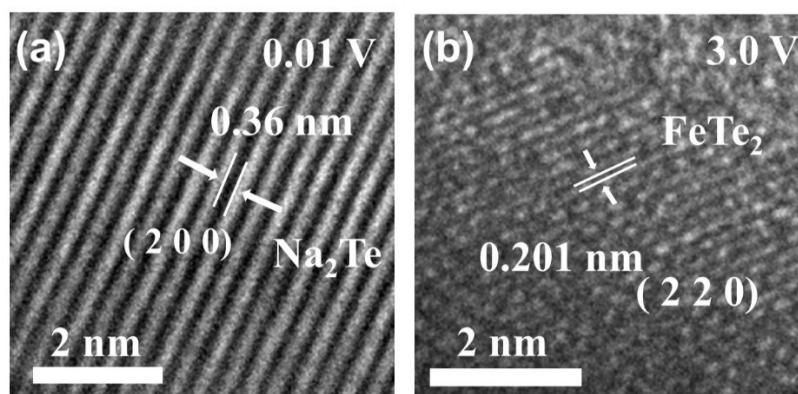


Fig. S13. Ex-situ HRTEM images of the FeTe₂/CNFs: (a) fully discharged to 0.01 V and (b) fully charged to 3.0 V.